

ELECTRIC AND MAGNETIC FIELD VARIATIONS AT LOW AND EQUATORIAL LATITUDES DURING SC, DP 2, AND Pi 2 EVENTS

K. YUMOTO, A. IKEDA, M. SHINOHARA and T. UOZUMI

*Space Environment Research Center and
Department of Earth and Planetary Sciences
Kyushu University, 6-10-1 Hakozaki, Higashi-ku
Fukuoka, 812-8581, Japan*

K. NOZAKI and S. WATARI

*National Institute of Information and Communication Technology
4-2-1 Nukui-Kitamachi, Koganei, Tokyo, 184-8795, Japan*

K. KITAMURA

*Department of Mechanic and Electrical Engineering
Tokuyama College of Technology, 3538 Kumetakajo
Shunan, 745-8585, Japan*

V. V. BYCHKOV and M. SHEVTSOV

*Institute of Cosmophysical Research and Radiowaves Propagation (IKIR)
Far Eastern Branch of Russian Academy of Sciences
684034 Kamchatka Region, Elizovskiy District
Paratunka, Mirmaya Str. 7, Russia*

Relations of ionospheric electric and magnetic fields at low and equatorial latitudes during SC, DP 2 and Pi2 events were investigated by analyzing the MAGDAS magnetic data and the Doppler data of our FM-CW ionospheric radar. From the analyses, we found that the ionospheric electric fields at lower latitudes during SC events consist of two components: one is the dawn-to-dusk electric field, which penetrates from the polar ionosphere into the day- and night-side equatorial ionospheres, and the other is the globally-westward electric field ($\delta\mathbf{E} = -\mathbf{v} \times \mathbf{B}_0$), which may be induced globally in the ionosphere or caused by a globally-earthward movement (\mathbf{v}) of the ionospheric plasmas. The H-component of DP 2 magnetic variation in the 10-nT range observed near the magnetic equator in nighttime shows roughly in-phase relation with those in daytime; however, it cannot be explained by the DP 2 dawn-to-dusk electric field observed at middle latitude in nighttime. A new generation mechanism is needed to interpret the globally coherent DP 2 magnetic variation near the magnetic equator. The compressional Pi 2 magnetic pulsation ($\delta\mathbf{B}$)

observed globally near the magnetic equator is found to show the relation of $\omega \delta \mathbf{B} = -\mathbf{k} \times \delta \mathbf{E}$ to the ionospheric Pi 2 electric field ($\delta \mathbf{E}$), where ω is the wave frequency, and the wave vector (\mathbf{k}) is directed earthward.

1. Introduction

The sudden increase of solar-wind dynamic pressure causes a sudden increase of the geomagnetic field especially at low latitudes. This phenomenon is called geomagnetic sudden commencement (SC). The disturbance field of SC is divided into two components¹:

$$D_{SC} = DL + DP,$$

where DL is the disturbance at low latitudes and represents a step-function like increase of the H-component magnetic field at low latitudes, while DP denotes the disturbance due to polar ionospheric current, and is dominant at high latitudes. DL is caused by the current circuit flowing on the compressed magnetopause and the propagating compressional hydromagnetic (HM) wave in the magnetosphere.² DP shows two-pulse magnetic structure caused by the polar ionospheric electric field:

$$DP = DP_{PI} + DP_{MI},$$

where PI denotes the preliminary impulse and MI denotes the following main impulse, and the two are driven by the dusk-to-dawn and dawn-to-dusk electric fields, respectively. These electric fields are believed to penetrate from the magnetosphere into the polar ionosphere,^{2,16} and instantaneously transmit into the low-latitude ionosphere by a TM (transverse magnetic) wave-guide mode.^{5,6}

DP 2 magnetic fluctuations are characterized by quasi-periodic variations with timescales of about 20 min to a few hours. DP 2 magnetic fluctuations appear coherently at high latitudes and at the dayside magnetic equator. Southward turnings of the interplanetary magnetic field (IMF) are believed to be the main cause of DP 2 fluctuations on the ground.^{8,9} The equivalent current system of DP 2 fluctuations consists of two vortices in the polar region, where the DP 2 dawn-to-dusk electric field penetrates instantaneously into the lower-latitude and the equatorial ionospheres.⁷ At the dayside magnetic equator, ionospheric current driven by the penetrating DP 2 electric field is amplified, because of the conductivity enhancement localized within a few degrees of the dip equator (i.e., the Cowling effect). Accordingly, magnetic DP 2 fluctuations show amplitude enhancement

at the dayside magnetic equator. By using this peculiarity, the dawn-to-dusk electric field in the ionosphere can be estimated from ground-based magnetic field observations. On the other hand, the ionospheric conductivity declines during nighttime. Therefore, the ionospheric current may not flow easily during the nighttime equatorial region. In this case, DP 2 electric field fluctuations in the ionosphere cannot be estimated from the magnetic observations. In order to measure the ionospheric electric fields in the nighttime, direct ionospheric observations by Frequency Modulated Continuous Wave (FM-CW) radar are needed.²²

Pi2 magnetic pulsations, impulsive hydromagnetic oscillations with a period of 40–150s, occur globally at the onset of the magnetospheric substorm expansion phase. From long-term observations, it has been found that ground Pi2 pulsations are mixtures of several components of reflecting (1) propagations of fast and shear Alfvén wave, (2) resonances of plasmaspheric/magnetospheric cavity and magnetic field lines, and (3) transformations to ionospheric current systems at low, middle, and high latitudes.^{12,21} However, it has been unclear how these components coupled with each other and how their signals are distributed at different latitudes. Recently, Tokunaga *et al.*¹⁷ explored the possibilities of identifying the global system of Pi2 pulsations by Independent Component Analysis (ICA). They have successfully decomposed an isolated Pi2 event on a quiet day observed at the CPMN stations into two components. One was the global oscillation that occurs from high to equatorial latitudes on the nightside with a common waveform, and has an amplitude maximum at high latitude. Another component was localized at high latitudes on the night side, whose amplitude was quite weak at low latitudes but was enhanced near the dayside magnetic equator.

The global generation and propagation mechanisms of these transient magnetic SC, DP 2, and Pi2 variations are not yet clarified sufficiently, because they have been discussed by using only magnetic field data. Therefore, global electric and magnetic field observations and studies are needed. In order to simultaneously measure ionospheric electric fields with magnetic fields of transient SC, DP 2, and Pi2 phenomena, and to understand how these phenomena propagate and/or penetrate globally and instantaneously from the outer magnetosphere into the lower-latitude ionosphere, the Space Environment Research Center (SERC) at Kyushu University is deploying a new MAGnetic Data Acquisition System (MAGDAS) in the Circum-pan Pacific Magnetometer Network (CPMN) region and a FM-CW radar chain at low- and mid-latitude stations along the 210° magnetic meridian (MM), as shown in Fig. 1.^{23,24}

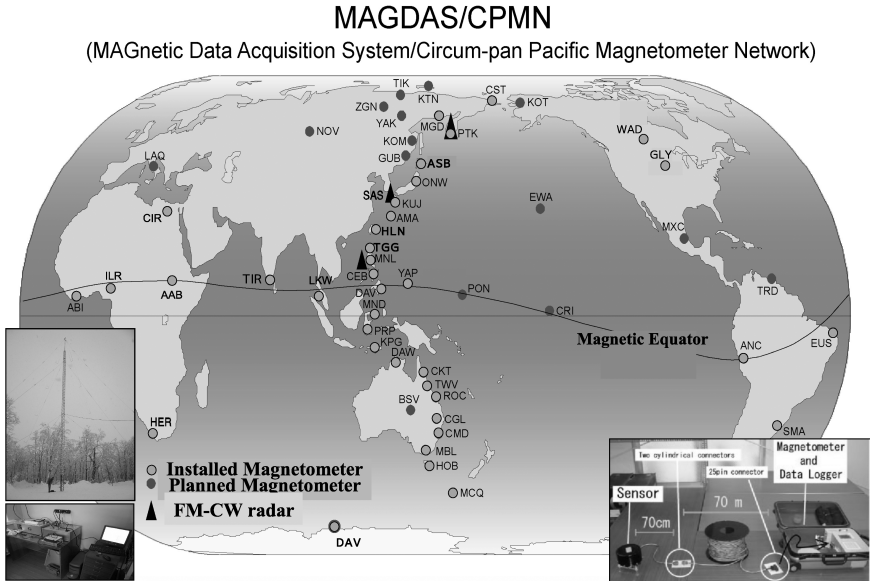


Fig. 1. MAGDAS/CPMN station map with MAGDAS magnetometer and FM-CW radar.

2. Magnetic and Electric Field Data Set

The Circum-pan Pacific Magnetometer Network (CPMN) was constructed by Kyushu University in collaboration with about 30 international organizations along the 210° MM and the magnetic equator, respectively, during the international Solar Terrestrial Energy Program (STEP) period (1990–1997).^{19–21} For space weather study and application, the SERC is now deploying a new real-time MAGnetic Data Acquisition System (MAGDAS) in the CPMN region, and a FM-CW radar array along the 210° MM. Fifty new fluxgate-type magnetometers and their data acquisition systems from Japan and overseas have been installed by the SERC since 2005.^{23,24} The horizontal (H)-, declination (D)-, and vertical (Z)-components of the ambient magnetic field are measured using field-canceling coils over the dynamic range of $\pm 64,000$ nT. The magnetic variations (δH , δD , δZ) subtracted from the ambient field components (H, D, Z) are further digitized by a 16-bit A/D converter. The resolution of MAGDAS/CPMN data is 0.031 nT/LSB in the ± 1000 nT range, and the estimated noise level of the magnetometers is less than 0.1 nTp-p.

In order to study SC and Pi 2 magnetic pulsations during 2002–2005, we analyzed 3-s averaged data from the CPMN stations at low latitudes, namely Kujyu (KUJ; M. Lat. 23.6° , M. Lon. 203.2°) and Kagoshima (KAG; 21.9° , 202.3°) in Japan, Pohnpei (PON; 0.08° , 229.19°) near the dip equator in the Pacific region, and Guadalupe (GLP; -0.06° , 355.57°) in Peru, and at high latitude, namely Tixie (TIK; 65.65° , 196.90°) in Russia. For the data gaps at KUJ, the data from a similar instrument at KAG were used. KUJ is about 100 km southeastward from the FM-CW radar site at Sasaguri, Fukuoka, Japan (SSG; 23.2° , 199.6°), and KAG is about 230 km southward from SSG. We also analyzed DP 2 magnetic variations observed at the MAGDAS stations at Ancon, Peru (ANC; 3.05° , 354.40°) and Santa Maria, Brazil (SMA; -19.27° , 13.29°) during daytime, and at Davao, the Philippines (-1.37° , 196.53°) during nighttime during April 2007.

In this chapter we analyzed the ionospheric data from our FM-CW radars located at Sasaguri, and Paratunka (PTK; 46.17° , 226.02°) in Kamchatka, Russia. The FM-CW radar is a type of HF (High Frequency) radar and can measure the range of target as well as its Doppler-related information. One application of the FM-CW radar is the technique developed by Barrick³ to measure sea scatter. The FM-CW radar for the Doppler observations was first put to practical use by Poole¹³ and Poole and Evans.¹⁴ Nozaki and Kikuchi^{10,11} made improvements to the FM-CW radar system. Our Doppler observations started at Sasaguri in November 2002, and at Paratunka in September 2006. From the Doppler mode observations of our FM-CW radar, we can measure vertical drift velocity and virtual height of ionospheric plasmas with high time resolution. Then, we can estimate the intensity of the ionospheric electric field. Furthermore, altitude information enables us to confirm whether the observed ionosphere is in the F-region. The sampling time of our radar system is 10 s.⁴

When the eastward electric field penetrates into the low-latitude ionosphere, the ionospheric plasma drifts upward owing to the frozen-in effect ($\mathbf{E} \times \mathbf{B}_0$ effect) in the F-region. On the other hand, the ionospheric plasma drifts downward when the westward electric field is applied into the ionosphere. Our radar system provides us with the Doppler frequency shift (Δf), that is the difference of transmitting frequency (f_0) and receiving frequency ($\Delta f + f_0$) of the radio wave reflected from the ionized layer, and a function of vertical movement of the ionized layer. The relational expression of Δf and f_0 is represented by $\Delta f = f_0 \times 2v/c$, where v is the vertical drift velocity, and c is the velocity of light. At Sasaguri we transmit radio waves of $f_0 = 8.0$ MHz during daytime and 2.5 MHz during

nighttime, because the ionospheric plasma density is higher during daytime than during nighttime. From the above relational expression, the vertical drift velocity (v) of the ionosphere is given by $c\Delta f/2f_0$. The accuracy of the vertical drift velocity is 1.5 m/s and 4.7 m/s for the transmitting frequency of 8.0 MHz and 2.5 MHz, respectively.

In addition, we can calculate the intensity of the ionospheric electric fields, by using the relation of $\mathbf{E} = \mathbf{v} \times \mathbf{B}_0$, where \mathbf{E} is roughly east-west electric field in the F-region, and \mathbf{B}_0 is the ambient magnetic field at Sasaguri. The \mathbf{B}_0 is given by the IGRF model (cf. <http://swdcwww.kugi.kyoto-u.ac.jp/index.html> at the World Data Center for Geomagnetism, Kyoto), which requires two inputs: (1) the altitude of the F-region (in this case, given by our radar), and (2) the geographical coordinates of Sasaguri (obtained from the GPS system).

3. Data Analyses of SC, DP 2, and Pi 2 Events

We have built a FM-CW radar (HF radar of 2–42 MHz) system at Sasaguri, Fukuoka. The height of dipole antenna is 26 m. HF radio wave of 2–30 MHz is emitted in the vertical direction with 20 W power in the ionosonde mode, while radio waves of central frequencies of $f_0 = 2.5$ and 8 MHz are emitted during nighttime (09–21 UT = 18–06 LT) and daytime (21–09 UT = 06–18 LT), respectively, in the Doppler mode. The speed of sweep frequency and the sampling frequency are 100–1000 kHz/s and 2000–20,000 Hz/s, respectively. This system can measure the Doppler frequency shift (Δf) of radio wave reflected from the ionized layer and the height of reflection layer at 10-s sampling rate, from which we can deduce the ionospheric electric fields associated with SC, DP 2, and Pi 2 events.

3.1. *Ionospheric electric fields and ground magnetic fields during SC events*

The upper panel of Fig. 2 shows SC magnetic variations at KUJ during daytime and at SMA during nighttime, and the associated ionospheric electric field observed at SSG during daytime on 4 November 2003. We can see eastward ionospheric electric field with 0.69 mV/m peak-to-peak intensity at SSG and step-like magnetic field variations of about 60 nT amplitude at both KUJ on the dayside and SMA on the nightside. The bottom panel of Fig. 2 shows the SC magnetic variation at KUJ and the ionospheric electric field at SSG observed during nighttime on

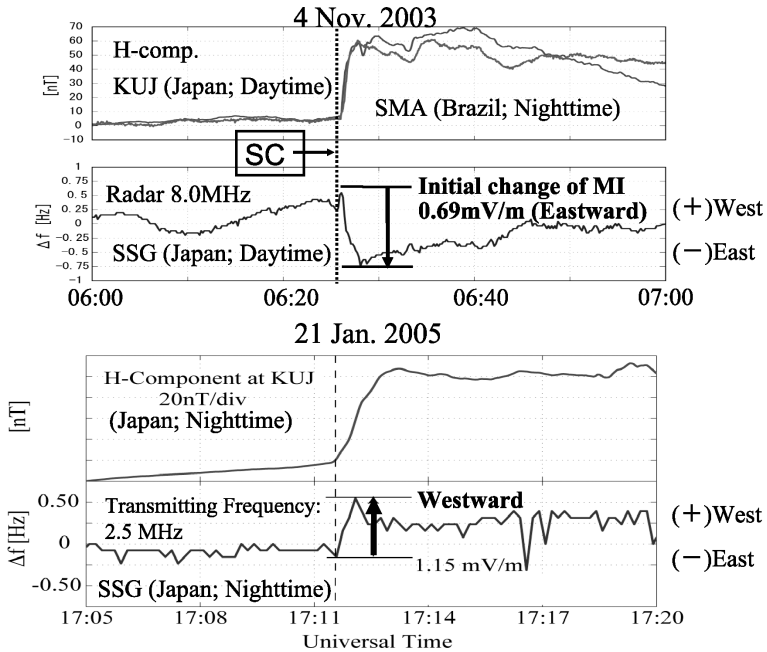


Fig. 2. (Upper) Dayside ionospheric electric SC field at SSG with magnetic variations at KUIJ during daytime and at SMA during nighttime on 4 November 2003. (Bottom) Nightside ionospheric electric SC field at SSG with magnetic variation at KUIJ during nighttime on 21 January 2005.

21 January 2005. In this case, westward ionospheric electric field of 1.15 mV/m peak-to-peak intensity was observed at SSG with step-like magnetic variation of 80 nT at KUIJ.

We selected 40 SC events that were identified using magnetic data from KUIJ and the FM-CW radar data during the period of 2002–2005. At first, we examined step-function-like magnetic changes, and then read the peak-to-peak intensity of the ionospheric electric fields during the SC events. We found that the ionospheric electric fields denote the direction eastward during daytime (06–20 LT) and westward during the nighttime (17–07 LT), as shown in Fig. 3. The averaged peak-to-peak intensity of observed electric fields is also found to be 0.5 mV/m during the daytime and 1.0 mV/m during the nighttime. This daytime and nighttime asymmetries of observed ionospheric electric fields cannot be interpreted using only the penetration model of polar dawn-to-dusk electric field into the day- and night-side lower ionosphere during the SC events. The scale size of changes

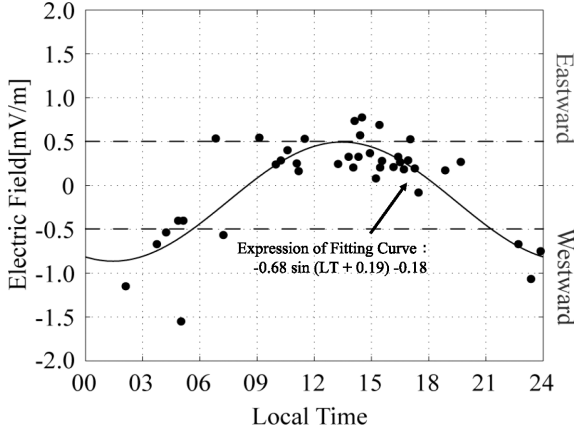


Fig. 3. Local-time dependence of ionospheric electric fields of SCs at Sasaguri during 2002–05.

in the solar wind is too large in comparison to that of the globe; therefore, the day–night asymmetry of the ionospheric electric fields in Fig. 3 must not be related to the solar-wind conditions. We may need additional electric field component or a local time-dependence of the penetration efficiency of the polar electric fields into the low-latitude ionosphere.

We compared the peak-to-peak intensity of ionospheric electric fields with the step-function-like change of magnetic fields during SC events, and found a clear correlation (correlation coefficient = 0.70) between the electric and magnetic fields. We also compared the peak-to-peak intensity of ionospheric electric fields with the dynamic pressure (P_{sw}) in the solar wind during the interplanetary shock events. There was a correlation (correlation coefficient = 0.65) between the two, while no correlation was found between the electric field intensity in the solar wind (E_{sw}) and the intensity of ionospheric electric fields. The ionospheric electric fields seem to depend mainly on the P_{sw} .

These observations suggest that the ionospheric electric fields at low latitudes during SC events consist of two components: one is the dawn-to-dusk electric field of averaged intensity of 0.75 mV/m, which penetrates from the polar ionosphere into the day- and night-side equatorial ionospheres, and the other is the globally-westward electric field ($\delta\mathbf{E} = -\mathbf{v} \times \mathbf{B}_0$) of averaged intensity of 0.25 mV/m. The second component may be a globally induced, westward electric field ($\delta\mathbf{E}$) in the ionosphere or may be caused by a globally-earthward movement (\mathbf{v}) of ionospheric plasmas during SC events.

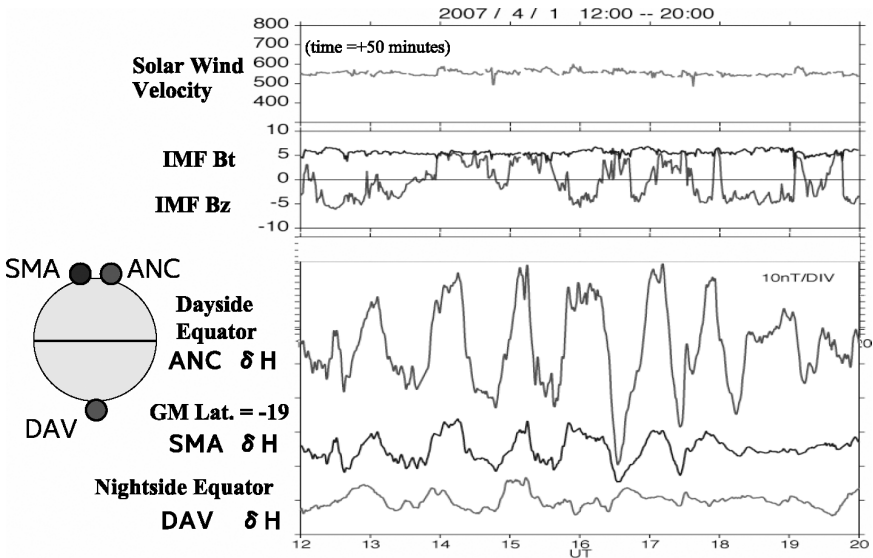


Fig. 4. DP 2-type IMF Bz variation at ACE in the solar wind (Upper), and H-component DP 2 variations observed by MAGDAS at ANC and SMA during daytime and at DAV during nighttime (Bottom) on 1 April 2007.

3.2. DP 2 ionospheric electric field and global magnetic field variations

The upper panel of Fig. 4 shows the solar-wind velocity and the total and z-component of interplanetary magnetic field (IMF) observed by the ACE satellite around the Lagrange point (L1) (see http://helios.gsfc.nasa.gov/ace_spacecraft.html); the data has been shifted by 50 min forward to take into account the solar-wind velocity and the ACE satellite location. The lower panel shows the H-component magnetic field variations observed by the MAGDAS magnetometer near the magnetic equator at ANC and at low latitude at SMA during daytime and near the magnetic equator at DAV during the nighttime on 1 April 2007. Noncompressional DP 2 fluctuation with about 1 h period can be seen only in the IMF Bz component at the ACE satellite. On the other hand, the H-component DP 2 magnetic variations on the ground indicate roughly in-phase relation at lower latitudes during daytime and nighttime. If the magnetic field variations were caused by penetration electric field associated with change in IMF Bz, the penetration electric field at the nightside should have an opposite direction to that at the dayside. In particular, the three pulses between 12

and 16 UT at DAV during the nighttime show a clear in-phase relation with the dayside DP 2 variations at low and equatorial latitudes, but the nighttime DP 2 magnetic variation at 16 to 20 UT might be shielded and reduced by the sub-storm effect (not shown in Fig. 4). Also a clear equatorial enhancement of DP 2 can be seen at ANC in daytime. We do not have a definitive interpretation for the in-phase variations of DP 2 magnetic fields at the dayside and nightside magnetic equator. More observations and new models are needed to understand the observations.

Figure 5 shows the H-component DP 2 magnetic variation observed by MAGDAS near ANC during daytime, and ionospheric DP 2 electric field measured by FM-CW radar at PTK at mid-latitude during nighttime. The equatorial enhancement of dayside DP 2 magnetic variation at ANC can be driven by an ionospheric eastward electric field, while the observed ionospheric westward electric field during the nighttime is synchronized with the DP 2 magnetic variation during daytime. This observation can be interpreted by a scenario in which the IMF B_z variation drives a dawn-to-dusk electric field in the solar wind, which penetrates into the polar region and transmits into both the day- and night-sides of the low-latitude ionosphere.

It is noteworthy that the H-component DP 2 magnetic variation observed near the magnetic equator during the nighttime indicates

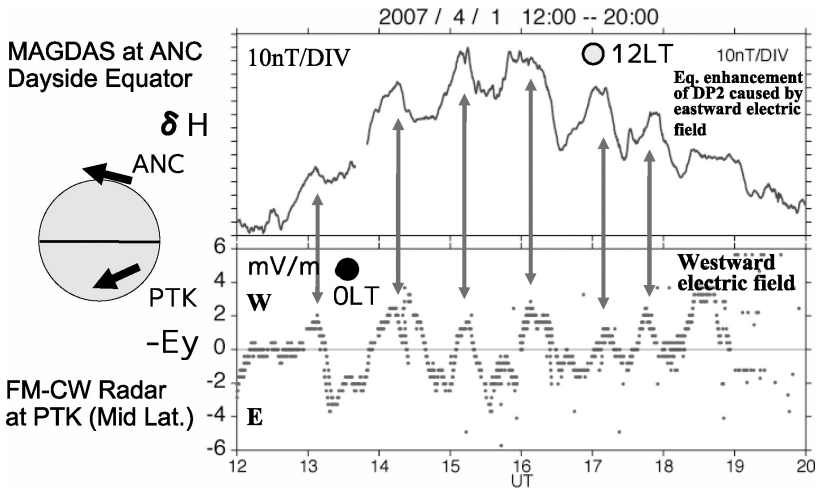


Fig. 5. H-component magnetic DP 2 variation observed by MAGDAS at ANC during daytime, and ionospheric electric DP 2 field observed by FM-CW radar at PTK during nighttime on 1 April 2007.

roughly in-phase relation with those during daytime, as shown in Fig. 4. However, the in-phase relation cannot be explained by using the decline in conductivity during the nighttime ionosphere with the ionospheric DP2 dawn-to-dusk electric field observed at PTK, as shown in Fig. 5. A new generation mechanism is needed to understand the globally coherent, DP2 magnetic variations near the magnetic equator.

3.3. Equatorial Pi 2 magnetic pulsations and ionospheric Pi 2 electric field

The left panel of Fig. 6 shows a typical magnetic substorm event, i.e. negative and positive bay variations with Pi2 pulsations observed at high (TIK), low (KUJ), and the equatorial (PON) latitudes on 6 November 2003. The middle panel shows the band-pass filtered amplitude-time records of H-component magnetic variations at TIK, KUJ, and PON during the nighttime and at GLP during daytime, and the ionospheric Pi2 electric pulsation observed by the FM-CW radar at SSG in the Doppler mode during the nighttime. We can see the equatorial enhancement of Pi2 magnetic amplitude at GLP during daytime and a globally coherent nature of Pi2 pulsations at GLP and PON near the magnetic equator, and at

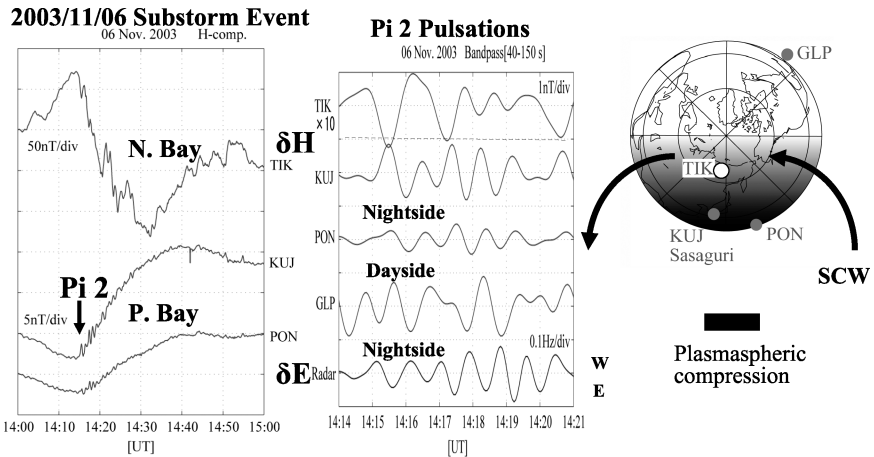
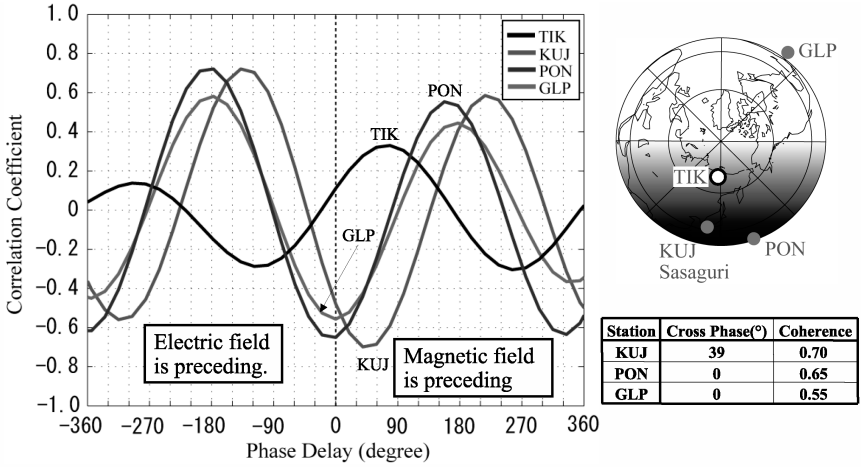


Fig. 6. Magnetic sub-storm, negative and positive bays at TIK, KUJ, and PON during nighttime (Left), Pi 2 magnetic pulsation at TIK, KUJ, PON during nighttime and at GLP during daytime, and ionospheric Pi 2 electric pulsation at SSG (Middle), and a schematic formation of sub-storm current wedge and plasma compression during the sub-storm expansion (Right).



The Pi 2 electric field oscillates with the equatorial magnetic fields (PON and GLP) in-phase. Where there is a phase delay between the electric field and magnetic field at low latitude KUJ.

Fig. 7. Cross correlation of Pi2 magnetic pulsations at TIK, KUJ, and PON during nighttime and at GLP during daytime with ionospheric Pi2 electric field at SSG during nighttime.

KUJ at low latitude. It is also found that the eastward electric field of ionospheric Pi2 at SSG indicates a nearly in-phase relation with the northward magnetic field of the global lower-latitude Pi2 pulsation.

Figure 7 shows the cross-correlation of the ionospheric Pi2 electric field pulsation observed at low latitude (SSG) during nighttime to Pi2 magnetic pulsation observed at high latitude (TIK), low latitude (KUJ), and magnetic equator (PON), respectively, during nighttime and at the magnetic equator (GLP) during daytime. The Pi2 magnetic pulsations at high (TIK) and low latitudes (KUJ), respectively, show a nearly out-of-phase relation. We can see a little bit of phase difference between Pi2 magnetic pulsations observed at the low-latitude station (KUJ) and those at the magnetic equator stations (PON, GLP). There is almost no phase delay between the eastward electric field (δE) at low-latitude station SSG during nighttime and the northward magnetic fields (δB) near the magnetic equator at GLP during daytime and at PON during nighttime. If the ionospheric conductivity is not negligible around the nighttime magnetic equator, the eastward electric field of Pi2 may drive the ionospheric current. Further, it can produce the northward magnetic field on the ground. In the case of the conductivity decline in the nighttime ionosphere, the global

compressional Pi 2 pulsation observed near the magnetic equator indicates a relation of $(\omega \delta \mathbf{B} = -\mathbf{k} \times \delta \mathbf{E})$, where ω is the wave frequency and the wave vector (\mathbf{k}) is directed earthward.

4. Discussion and Conclusion

In order to measure ionospheric electric fields simultaneously with magnetic fields of transient SC, DP 2, and Pi 2 phenomena, and to understand how these phenomena propagate and/or penetrate globally from the outer magnetosphere into the lower-latitude ionosphere, the SERC at Kyushu University is now deploying a new MAGDAS in the CPMN region and a FM-CW radar chain along the 210°MM. From the MAGDAS/CPMN observations, the following electromagnetic characteristics of SC, DP 2, and Pi 2 events are found:

- (1) The ionospheric electric fields at lower latitudes during SC events consist of two components: one is the dawn-to-dusk electric field of averaged 0.75 mV/m peak-to-peak intensity, which penetrates from the polar ionosphere into the day- and night-side equatorial ionospheres, and the other is the globally-westward electric field ($\delta \mathbf{E} = -\mathbf{v} \times \mathbf{B}_0$) of averaged 0.25 mV/m peak-to-peak intensity, which may be induced globally in the ionosphere or caused by a globally-earthward movement (\mathbf{v}) of the ionospheric plasmas.
- (2) The H-component DP 2 magnetic variation of 10 nT observed near the magnetic equator during nighttime shows roughly an in-phase relation with those during daytime, but it cannot be explained on the basis of the ionospheric DP 2 dawn-to-dusk electric field and the conductivity decline during the nighttime ionosphere. A new generation mechanism is needed to understand the globally coherent, DP 2 magnetic variation near the magnetic equator.
- (3) The global compressional Pi 2 magnetic pulsation ($\delta \mathbf{B}$) observed near the magnetic equator is found to show a relation of $(\omega \delta \mathbf{B} = -\mathbf{k} \times \delta \mathbf{E})$ to the ionospheric Pi 2 electric pulsation ($\delta \mathbf{E}$), where ω is the wave frequency and the wave vector (\mathbf{k}) is directed earthward.

From multi-satellite and ground magnetic field observations, Wilken *et al.*¹⁸ proposed that the compressional HM wave-front can propagate to the nightside magnetosphere and ionosphere at the time of SC. In a recent study on SC-related electric and magnetic field perturbations in 126 SC

events measured by the Akebono satellite, Shinbori *et al.*¹⁵ reported that the initial electric field excursion is directed westward in the entire region of the inner magnetosphere and plasmasphere within an L-value range from 1.08 to 4.5. The intensity was in a range from 0.2 to 40 mV/m, and did not show a clear dependence on magnetic local time. Moreover, the duration of the initial electric field excursion is about 64–120 s. They also concluded that the westward electric field is an inductive field created by compressional HM wave. In the present chapter, the ionospheric electric fields observed by our FM-CW radar system at lower latitude during SC events are found to consist of two components: one is the dawn-to-dusk electric field of the Main Impulse (DP_{MI}), and the other is the globally-westward electric field ($\delta\mathbf{E} = -\mathbf{v} \times \mathbf{B}_0$), which may be induced globally in the ionosphere or caused by a globally-earthward movement (\mathbf{v}) of the ionospheric plasmas. These electric fields, which are induced globally in the ionosphere and/or due to globally-earthward movement of the ionospheric plasma, must be associated with the westward electric fields observed by the Akebono satellite.¹⁵

The H-component DP 2 magnetic variation observed near the magnetic equator during nighttime, as shown in Fig. 4, indicates roughly an in-phase relation with those during daytime. However, the observed magnetic DP 2 variations during nighttime cannot be explained by using the ionospheric DP 2 dawn-to-dusk electric field with the conductivity decline during the nighttime ionosphere. In order to understand the globally coherent, DP 2 magnetic variations near the magnetic equator, and to make a new generation model for the global DP 2 at the magnetic equator, we need more coordinated magnetic and electric field observations. For example, we can examine if the DP 2 magnetic fluctuations on the ground are driven by and/or associated with dynamic pressure changes in the solar wind and compressional variations in the magnetosphere.

Ground Pi 2 pulsations are mixtures of several components reflecting propagations of fast and shear Alfvén waves, the resonances of the magnetospheric cavity and magnetic lines of force, and transformations to the ionospheric current systems with penetrations of ionospheric electric field variations from high to equatorial latitudes.^{12,21} However, there are still open questions how they couple to each other, how these signals distribute at different latitudes, and how global-mode oscillations from high to equatorial latitudes and during day- and night-time can be generated (and/or excited). We need more globally-coordinated magnetic and electric field observations and theoretical works.

Acknowledgments

The authors would like to thank Mr Ishihara, Mr Mori and Mr Shinbaru for their contributions to the construction of our FM-CW radar system. The host scientists at ANC and GLP in Peru, at SMA in Brazil, and at PON in Federated States of Micronesia are Dr T Ishitsuka, Prof Nelson J Schuch, and Prof H Utada, respectively. We also acknowledge Dr Shinbori for providing us with the SC-event list and for useful discussion. One of the authors (A Ikeda) is supported by the Professor Tatsuro Matsumoto Scholarship Fund. The PI of MAGDAS/CPMN project, K Yumoto, SERC, Kyushu University very much appreciates the 30 organizations and co-investigators around the world for their ceaseless cooperation and contribution to the MAGDAS/CPMN project. Financial supports were provided by Japan Society for the Promotion of Science (JSPS) as Grant-in-Aid for Overseas Scientific Survey (15253005, 18253005) and for publication of scientific research results (188068).

References

1. T. Araki, *Planet. Space Sci.* **25** (1977) 373–384.
2. T. Araki, in *Solar Wind Sources of Magnetospheric Ultra-Low-Frequency Waves*, eds. M. J. Engebretson *et al.*, *Geophys. Monogr. Ser.*, Vol. 81 (AGU, Washington, DC, 1994), pp. 183–200.
3. D. E. Barrick, *NOAA Technical Report ERL 283-WPL 26* (1973).
4. A. Ikeda, K. Yumoto, M. Shinohara, K. Nozaki, A. Yoshikawa and A. Shinbori, *Mem. Fac. Sci., Kyushu Univ., Ser. D, Earth Planet. Sci.* **XXXII**(1) (2008) 1–6.
5. T. Kikuchi and T. Araki, *J. Atmos. Terr. Phys.* **41** (1979) 917–925.
6. T. Kikuchi, *J. Geophys. Res.* **91** (1986) 3101.
7. T. Kikuchi, H. Luhr, T. Kitamura, O. Saka and K. Schlegel, *J. Geophys. Res.* **101** (1996) 17161.
8. A. Nishida, *J. Geophys. Res.* **73** (1968) 1795.
9. A. Nishida, *J. Geophys. Res.* **73** (1968) 5549.
10. K. Nozaki and T. Kikuchi, *Mem. Natl. Inst. Polar Res.*, Spec. Issue **47** (1987) pp. 217–224.
11. K. Nozaki and T. Kikuchi, *Proc. NIPR Symp. Upper Atmos. Phys.* **1** (1988) 204–229.
12. J. V. Olson, *J. Geophys. Res.* **104** (1999) 17,499–17,520.
13. A. W. V. Poole, *Radio Sci.* **20** (1985) 1609.
14. A. W. V. Poole and G. P. Evans, *Radio Sci.* **20** (1985) 1617.
15. A. Shinbori, T. Ono, M. Iizima and A. Kumamoto, *Earth Planet Space* **56** (2004) 269–282.
16. T. Tamao, *Rep. Ionos. Space Res. Jpn.* **18** (1964) 16–31.

17. T. Tokunaga, H. Kohta, A. Yoshikawa, T. Uozumi and K. Yumoto, *Geophys. Res. Lett.* **34** (2007) L14106, doi: 10.1029/2007GL030174.
18. B. Wilken, C. K. Goertz, D. N. Baker, P. R. Higbie and T. A. Fritz, *J. Geophys. Res.* **87** (1982) 5901–5910.
19. K. Yumoto and the 210° MM Magnetic Observation Group, *J. Geomag. Geoelectr.* **47** (1995) 1197–1213.
20. K. Yumoto and the 210° MM Magnetic Observation Group, *J. Geomag. Geoelectr.* **48** (1996) 1297–1309.
21. K. Yumoto and the CPMN Group, *Earth Planets Space* **53** (2001) 981–992.
22. K. Yumoto, M. Shinohara, K. Nozaki, E. A. Orsco, Fr. V. Badillo, D. Bringas and the CPMN and WestPac Observation Groups, in *COSPAR Colloquia Ser. Vol. 12, Space Weather Study using Multipoint Techniques*, eds. Ling-Hsiao Lyu (Elsevier Science Ltd, 2002), pp. 243–247.
23. K. Yumoto and the MAGDAS Group, in *Solar Influence on the Heliosphere and Earth's Environment: Recent Progress and Prospects*, eds. N. Gopalswamy and A. Bhattachayya (2006), IBN-81-87099-40-2, pp. 399–405.
24. K. Yumoto and the MAGDAS Group, *Bull. Astron. Soc. Ind.* **35** (2007) 511–522.